Two-pattern compound photonic crystals with a large complete photonic band gap

Lin Jia and Edwin L. Thomas

Phys. Rev. A **84**, 033810 — Published 8 September 2011

DOI: 10.1103/PhysRevA.84.033810

2-Pattern Compound Photonic Crystals with A Large, Complete Photonic Band Gap

*Lin Jia and Edwin L. Thomas**

Institute for Soldier Nanotechnologies, Department of Materials Science and Engineering,

Massachusetts Institute of Technology, Cambridge, Massachusetts 02139

E-mail: elt@mit.edu

Abstract:

We present a novel set of two-dimensional (2D) aperiodic structures with a large, complete photonic band gap (PBG), which are named "2-pattern photonic crystals". By superposing two sub-structures without regards to registration, we designed six new aperiodic PBG structures having complete PBG larger than 15% for $\varepsilon_2/\varepsilon_1 = 11.4$. The rod-honeycomb 2-pattern photonic crystal provides the largest complete PBG to date. For the first time, an aperiodic structure becomes the champion structure with the largest PBG. Surprisingly, the TM and TE gaps of a 2-pattern photonic crystal are much less interdependent than the PBGs of conventional photonic crystals proposed before, affording interesting capabilities for us to tune the TM and TE PBGs separately. By altering the respective sub-structures, optical devices for different polarizations (TE, TM or both) can be readily designed.

PACS: 42.70.Qs, 78.67.Pt, 07.05.Tp; 78.20.Bh; 42.70.-a

Photonic crystals, discovered in 1987 [1, 2], have attracted great interest due to their ability to control the flow of light [3-12]. A large number of PBG structures have been developed during the past twenty years. Up to now, all PBG structures can be categorized into three types: periodic structures [1, 13-24], quasicrystals [25-27] (exhibiting higher rotational symmetries than consistent with conventional periodic lattices), and even disordered structures [2, 28-30] with short range order. The 2-pattern photonic crystals reported here do not belong to any of these known categories and create a new fourth category: incommensurate compound crystals. Moreover**,** it is generally believed that high symmetry is a crucial ingredient in order to form a large PBG. The 2-pattern photonic crystals exhibit an outstanding complete band gap but do not have global or even local symmetries. Physical insights to the PBG properties of these 2-pattern photonic crystals are provided.

In our approach, we create a superior 2-pattern photonic crystal by combining a TM sub-structure having discrete dielectric features that provide a large TM PBG with a TE sub-structure having expanded dielectric features chosen to provide a large TE PBG. The sub-structures can be periodic or aperiodic. Our concept is based on the rationale that the TE sub-structure of the 2-pattern photonic crystal can be assumed a type of geometrical perturbation to the TM sub-structure and vice versa. A random perturbation of a given structure shrinks the size of the PBG, but the PBG is generally more robust to an ordered perturbation [31]. If the TE sub-structure filling ratio is not high, the ordered

geometrical perturbation does not strongly modify the TM PBG of the 2-pattern photonic crystal. Further, the small or zero TM PBG of the TE sub-structure brings trivial impact on the TM PBG of the 2-pattern photonic crystal which arises predominately from the TM sub-structure. The reverse situation holds for the TE PBG of the 2-pattern photonic crystal arising predominately from the TE sub-structure. Importantly, one photonic crystal is comprised of two superposed patterns, while previously reported photonic crystals are based on a single pattern. The TE and TM PBGs of 2-pattern photonic crystals are much less interdependent than the PBGs of conventional photonic crystals. Importantly, by selectively creating defects in the different sub-structures, we can design photonic devices for particular polarizations (TM, TE, or both).

To analyze the photonic band gap, we calculate the normalized density of states (DOS) via finite-difference time-domain (FDTD) [32, 33]. We assign a radiating dipole near the middle of a large portion of the structure and provide a perfectly matched layer (PML) on the boundaries. Four hundred detectors are distributed near the boundary of the simulated area to collect the transmission spectra, which represents the DOS. The calculation results are tested for different radiating dipole positions and radiating sources of a group of random distributed dipoles.

In 2D, the following factors define the 2-pattern photonic crystal: the morphology, the filling ratios, and the relative scale, position and orientation of the sub-structures. The first design factor is the morphology of the sub-structures. Here it is desirable to

select one structure with a large TE PBG but trivial TM PBG and another structure with a large TM PBG but trivial TE PBG. Throughout we assume that the dielectric material is GaAs with a permittivity of 11.4. We pick three candidates for the TM PBG sub-structure: rods on a triangular lattice (R-p6mm), (see Figure 1a, the current champion structure with the largest 47.3% TM PBG [34], and no TE PBG for 0.1 filling ratio), rods on a square lattice (R-p4mm) (see Figure 1b, 37.5% TM PBG and no TE PBG for 0.15 filling ratio), and an eight-fold quasicrystal of dielectric rods generated from hyperspace projection (QC-8mm) (see Figure 1c, 42.1% TM PBG and no TE PBG for ~ 0.1 filling fraction with $r/a = 0.185$, here r is the radius of the rods and a is the quasicrystalline length parameter). The two candidates for the TE PBG sub-structure both have p6mm symmetry: the connected honeycomb structure (HC-p6mm) (see Figure 1d, the current champion TE gap structure with the largest 42.5% TE PBG [35], and no TM PBG for 0.189 filling ratio) and circular rings on a triangular lattice (CR-p6mm) (see Figure 1e, 23.4% TE PBG and TM PBG less than 10% for 0.11 filling ratio).

The second design factor is the relative length scale of the two sub-structures. If we tune the scale of the TE (TM) sub-structure, the position of the TE (TM) PBG is shifted accordingly. The central frequency of the TE (TM) PBG is proportional to $1/a$, here a is the characteristic scale of the sub-structure [6]. For the TM sub-structure consisting of rods, the TM gap mainly comes from Mie resonance. As we increase the scale of the sub-structure, the radius of the rods increases, which leads to a lower Mie

resonance frequency and lower central gap frequency. An example is shown in Figure 2a, made from the superposition of the R-p4mm and CR-p6mm structures depicted in Figure 1b and Figure 1e. The filling ratio of the TE sub-structure is 0.102 and the filling ratio of the TM sub-structure is 0.149. The DOS plot for $a(TM)/a(TE) = 0.559$ is shown in Figure 2b. Note that the TE-PBG and the TM-PBG barely overlap. To maximize the complete PBG, we increase the periodicity of the TM sub-structure to decrease the central frequency of the TM-PBG. The tuning is continued until the TE-PBG and the TM-PBG fully overlap, which is shown in Figure 2c, leading to a complete PBG of 15%.

The third design factor is the individual sub-structure filling ratio. The filling ratio of each type of sub-structure controls the respective TE or TM gap but also modifies the strength of the ordered geometrical perturbation on the PBG of the other sub-structure. Therefore, altering the TE sub-structure can in general shrink the size of the TM PBG and the shrinkage will increase with the filling ratio of TE sub-structure while the reverse situation holds for varying the filling ratio of the TM sub-structure. The above effect has also been observed in a disordered system [30]. An example of the effect of filling ratio on the band gap is evident from the superposition of the R-p6mm and HC-p6mm crystals shown in Figure 3a. In Figure 3b, we fix the filling ratio of the TM sub-structure to 8.6% and increase the filling ratio of TE sub-structure. If the filling ratio of the TE sub-structure is too high (above 14%), the TM PBG is destroyed and the complete PBG closes. If the filling ratio of the TE sub-structure is too low (below 3%), the TE PBG of

the 2-pattern photonic crystal is low or even closes, which is also obviously disadvantageous. Therefore, the filling ratios of the sub-structures need to be adjusted carefully to maximize the complete PBG. In Figure 3c, the TE-PBG is smaller than TM-PBG and the complete PBG size is determined by the TE-PBG. To maximize the complete PBG, it is necessary to increase the TE-PBG size. Therefore we increase the filling ratio of the TE sub-structure. Although the TM-PBG shrinks because of this tuning, as shown in Figure 3b, the complete PBG size increases. We increase the filling ratio until the TE-PBG and TM-PBG match, which is shown in Figure 3d. The complete PBG is maximized because if the filling ratio of the TE sub-structure increases further, as shown in Figure 3e, the TM-PBG is smaller than the TE-PBG and the complete PBG is determined by the TM-PBG, which is relatively smaller than the complete PBG in Figure 3d.

The fourth and the fifth design factors are the relative position and orientation of the sub-structures. Interestingly, it turns out these factors have essentially no influence on the PBG since the changes in the relative location of the TE pattern, as an ordered geometrical perturbation to TM pattern, should not substantially vary the TM PBG of the 2-pattern photonic crystal with the same reasoning for the behavior of the TE PBG by the presence of the TM pattern. Therefore, the relative position and orientation of the TE/TM sub-structures only bring minor impact on the complete PBG, as confirmed in Figure 4 and Figure 5. The above fact is advantageous for the fabrication of the 2-pattern photonic crystals because it is not necessary to precisely adjust the relative position/orientation of

the two patterns.

Controlling electromagnetic waves at terahertz (THz) and gigahertz (GHz) frequencies is important and fabrication of 2-pattern photonic crystals at the associated length scales (microns and mm) is easy. Experimental techniques that can be used to fabricate "2-pattern photonic crystals" for the visible and near IR frequency regimes include nanoimprint lithography [36], electron beam lithography (EBL) [37], and focused ion beam lithography (FIBL). The 2-pattern photonic crystals are reasonably tolerant to possible experimental errors, including the variations of air gaps between dielectric regions. For example, for the structure shown in Figure 6(a), we introduced a 40% random variation in the diameter of the rods ($r = r_0 + \triangle r_0$, here $\triangle r_0$ is a random value between $[0.4r_0, -0.4r_0]$) and 40% random variation in the thickness of the honeycomb walls ($h = h_0 + \triangle h_0$, here $\triangle h_0$ is a random value between $[0.4h_0, -0.4h_0]$), and the complete PBG is still large: 16%. Furthermore, we also introduced 30% random variation in the positions of rods ($\vec{r} = \vec{r}_0 + \triangle \vec{r}_0$, here $|\triangle \vec{r}_0|$ is a random value between $[0.3a(TM), -0.3a(TM)]$) and the complete PBG is 15%.

For the three selected TE sub-structures and the two TM sub-structures shown in Figure 1, six 2-pattern photonic crystals can be constructed. For each combination, we maximize the complete PBG size by tuning the filling ratios and the relative scale of the sub-structures. The optimized structures with their discrete Fourier transforms (DFT) and

the associated DOS calculations are shown in Figure 6. The six optimized 2-pattern photonic crystals all have a complete PBG above 15% although as composite structures they do not possess *any* 2D symmetry. The aperiodic structure depicted in Figure 6(a) has the best complete PBG (20.4%), which is highest reported complete PBG for 2D structures. Surprisingly, an aperiodic structure now becomes the champion PBG structure. The optimized structures generally have almost equal sub-structure filling ratios (around 0.1) and the length scales of the sub-structures need to be similar.

Because the TM/TE PBGs of the 2-pattern photonic crystals each arise from one of the two patterns, by purposely introducing defects into the sub-structures, novel types of photonic devices for different polarizations (TE, TM or both) can be readily designed. For example, the waveguide in Figure 7(a) is created by removing features from the TE sub-structure without modifying the TM sub-structure. This waveguide only allows the propagation of TE waves and stops the propagation of TM waves. The waveguide in Figure 7(c) is created by removing only features from the TM sub-structure, allowing the propagation of TM waves and stopping TE waves.

In summary, a novel set of aperiodic PBG structures named "2-pattern photonic crystals" consisting of two sub-structures have been investigated. They do not belong to any of known PBG structure categories and create a new category: incommensurate compound photonic crystals. Surprisingly, these new photonic crystals do not possess any symmetry but they exhibit a large, complete PBG. Our work opens a wide range of

future opportunities. First, a rich variety of different 2-pattern photonic crystals can be developed using the large inventory of existing photonic crystals with sizeable TM or TE gaps. We anticipate that our method will become a useful tool to design photonic crystals with large, complete PBGs, which is essential for the associated photonic devices. Secondly, our work shows that the impact of symmetry on the PBG needs further investigation. Here we show that structures without any global crystallographic symmetry can have a complete PBG size larger than any of the present, highly symmetric 2D photonic crystals/quasicrystals. Finally, we demonstrate that the TE and TM PBGs of a 2-pattern photonic crystal can be tuned much more independently than conventional photonic crystals. By introducing defects into the sub-structures, photonic devices for TM/TE polarizations can be realized to achieve functionality not possible or highly challenging for conventional photonic crystal devices.

Acknowledgments:

We thank Professors J. Joannopoulos, E. Yablonovitch L. Kimerling, S. Johnson, and Dr. M. Maldovan for their helpful advice. This research is partially supported by the US Army Research office through the Institute for Soldier Nanotechnologies, under contract W911NF-07-D-0004 and by the National Science Foundation grant DMR 0804449.

Figure 1: The set of individual sub-structures and their corresponding PBGs (as indicated by the grey bands in the DOS plots). Three sub-structures with large TM PBG (rods on triangular lattice, rods on square lattice and rods decorating an eight-fold quasicrystal) are shown in (a) through (c). The filling ratios (f) of the sub-structures are dependent on r/a, where r is the radius of the rods and a is the appropriate lattice parameter. Two sub-structures with large TE PBG (the honeycomb structure and rings on a triangular lattice) are shown in (d) and (e) along with their corresponding DOS calculations.

Figure 2: Tuning the photonic band gap by altering the relative scale of sub-structures. (a): 2-pattern photonic crystal from the R-p4mm plus Cr-p6mm sub-structures. (b): The DOS plot for $a(TM)/a(TE) = 0.559$. (c): The DOS plot for $a(TM)/a(TE) = 0.656$.

Figure 3: Tuning the photonic band gap by altering the filling ratios of sub-structures. (a): 2-pattern photonic crystal from the superposition of the R-p6mm plus HC-p6mm. (b): The TE PBG and the TM PBG of the 2-pattern photonic crystal for different filling ratios of TE sub-structure. (c): DOS plot for TE sub-structure filling ratio $f(TE) = 0.058$. (d): DOS plot for $f(TE) = 0.086$. (e): DOS plot for $f(TE) = 0.114$.

Figure 4: The PBG for the R-p6mm plus HC-p6mm structure is robust for different superposition positions. (a): Four 2-pattern photonic crystals corresponding to different relative positions of the sub-structures are shown. The relative position brings trivial impact on the complete PBG, which is shown in (b).

Figure 5: The PBG for the R-p6mm plus HC-p6mm structure is robust to different superposition orientations. (a): Six 2-pattern photonic crystals corresponding to different relative orientations of the sub-structures are shown. The relative orientation brings trivial impact on the complete PBG, which is shown in (b).

Figure 6: Optimized 2-pattern photonic crystals with large, complete PBGs. (a): Champion structure based on the R-p6mm plus HC-p6mm sub-structures with $f(TE) = 0.086$ and $f(TM) = 0.086$ and $a(TM)/a(TE) = 0.7157$. The discrete Fourier transform (DFT) of the 2-pattern photonic crystal and the corresponding DOS calculation are shown below. (b): The 2-pattern photonic crystal from the R-p4mm plus HC-p6mm sub-structures with $f(TE) = 0.08$, $f(TM) = 0.14$ and $a(TM)/a(TE) = 0.67$. (c): The 2-pattern photonic crystal from the QC-8mm plus HC-p6mm sub-structures with $f(TE) = 0.11$ and $r/a = 0.22$. (d): The 2-pattern photonic crystal from the R-p6mm plus Cr-p6mm sub-structures with $f(TE) = 0.121$, $f(TM) = 0.102$ and $a(TM)/a(TE) = 0.7258$. (e): The 2-pattern photonic crystal from the R-p4mm plus Cr-p6mm sub-structures with $f(TE) = 0.108$, $f(TM) = 0.149$ and $a(TM)/a(TE) = 0.6563$. (f): The 2-pattern photonic crystal from the QC-8mm plus Cr-p6mm sub-structures with $f(TE) = 0.084$ and $r/a = 0.189$.

Figure 7 Waveguide devices in a 2-pattern photonic crystal. (a): a TE waveguide is created by removing TE sub-structure features from R-p6mm plus HC-p6mm structure. (b): TE wave intensity propagating in the waveguide while TM waves are blocked. (c): a TM waveguide is created by removing features from the TM sub-structure in the R-p6mm plus HC-p6mm structure. (d): TM wave intensity propagating in the waveguide while TE waves are blocked.

[1] E. Yablonovitch, Physical Review Letters **58**, 2059 (1987).
[2] S. John, Physical Review Letters **58**, 2486 (1987).
[3] E. Yablonovitch, T. J. Gmitter, and K. M. Leung, Physical Review Letters **67**, 2295 (1991).
[4] J. D. Joannopoulos, P. R. Villeneuve, and S. H. Fan, Nature **386**, 143 (1997).
[5] M. Maldovan, and E. L. Thomas, *Periodic Materials and Interference Lithography* (Wiley-VCH Verlag Gmbh& Co. KGaA Weinheim, 2009).
[6] J. D. Joannopoulos *et al.*, *Photonic crystals: molding the flow of light* (Princeton University Press, Princeton, 2008).
[7] S. H. Fan, and J. D. Joannopoulos, Physical Review B **65** (2002).
[8] S. H. Fan, Physica B-Condensed Matter **394**, 221 (2007).
[9] S. H. Fan *et al.*, Journal of Lightwave Technology **24**, 4493 (2006).
[10] O. Sigmund, Structural and Multidisciplinary Optimization **33**, 401 (2007).
[11] P. I. Borel *et al.*, Optics Express **12**, 1996 (2004).
[12] R. Matzen, J. S. Jensen, and O. Sigmund, Journal of the Optical Society of America B-Optical Physics **27**, 2040.
[13] G. Q. Liang *et al.*, Advanced Materials **22**, 4524.
[14] Y. Yin, Z. Y. Li, and Y. Xia, Langmuir **19**, 622 (2003).
[15] F. Wen *et al.*, Optics Express **16**, 12278 (2008).
[16] R. L. Chern, C. C. Chang, and R. R. Hwang, Physical Review E **68** (2003).
[17] M. Campbell *et al.*, Nature **404**, 53 (2000).
[18] A. Blanco *et al.*, Nature **405**, 437 (2000).
[19] E. Yablonovitch, Journal of the Optical Society of America B-Optical Physics **10**, 283 (1993).
[20] S. Noda *et al.*, Science **289**, 604 (2000).
[21] S. G. Johnson *et al.*, Physical Review B **60**, 5751 (1999).
[22] Y. Xu *et al.*, Chemistry of Materials **20**, 1816 (2008).
[23] X. L. Zhu, Y. G. Xu, and S. Yang, Optics Express **15**, 16546 (2007).
[24] X. L. Zhu *et al.*, Journal of the Optical Society of America B-Optical Physics **27**, 2534.
[25] Y. S. Chan, C. T. Chan, and Z. Y. Liu, Physical Review Letters **80**, 956 (1998).
[26] X. D. Zhang, Z. Q. Zhang, and C. T. Chan, Physical Review B **63** (2001).
[27] M. Florescu, S. Torquato, and P. J. Steinhardt, Physical Review B **80** (2009).
[28] Z. Y. Li, and Z. Q. Zhang, Advanced Materials **13**, 433 (2001).
[29] Z. Y. Li, X. D. Zhang, and Z. Q. Zhang, Physical Review B **61**, 15738 (2000).
[30] M. Florescu, S. Torquato, and P. J. Steinhardt, Proceedings of the National Academy of Sciences of the United States of America **106**, 20658 (2009).
[31] R. Biswa, I. kady, and K. Ho, Photonics and Nanostructures-Fundamentals and Applications **1**, 15 (2003).
[32] W. S. Kim, L. Jia, and E. L. Thomas, Advanced Materials **21**, 1921 (2009).
[33] S. G. Johnson, and J. D. Joannopoulos, Optics Express **8**, 173 (2001).
[34] M. C. Rechtsman *et al.*, Physical Review Letters **101** (2008).
[35] O. Sigmund, and K. Hougaard, Physical Review Letters **100** (2008).
[36] S. Y. Chou, P. R. Krauss, and P. J. Renstrom, Journal of Vacuum Science & Technology B **14**, 4129 (1996).
[37] Y. N. Xia *et al.*, Chemical Reviews **99**, 1823 (1999).

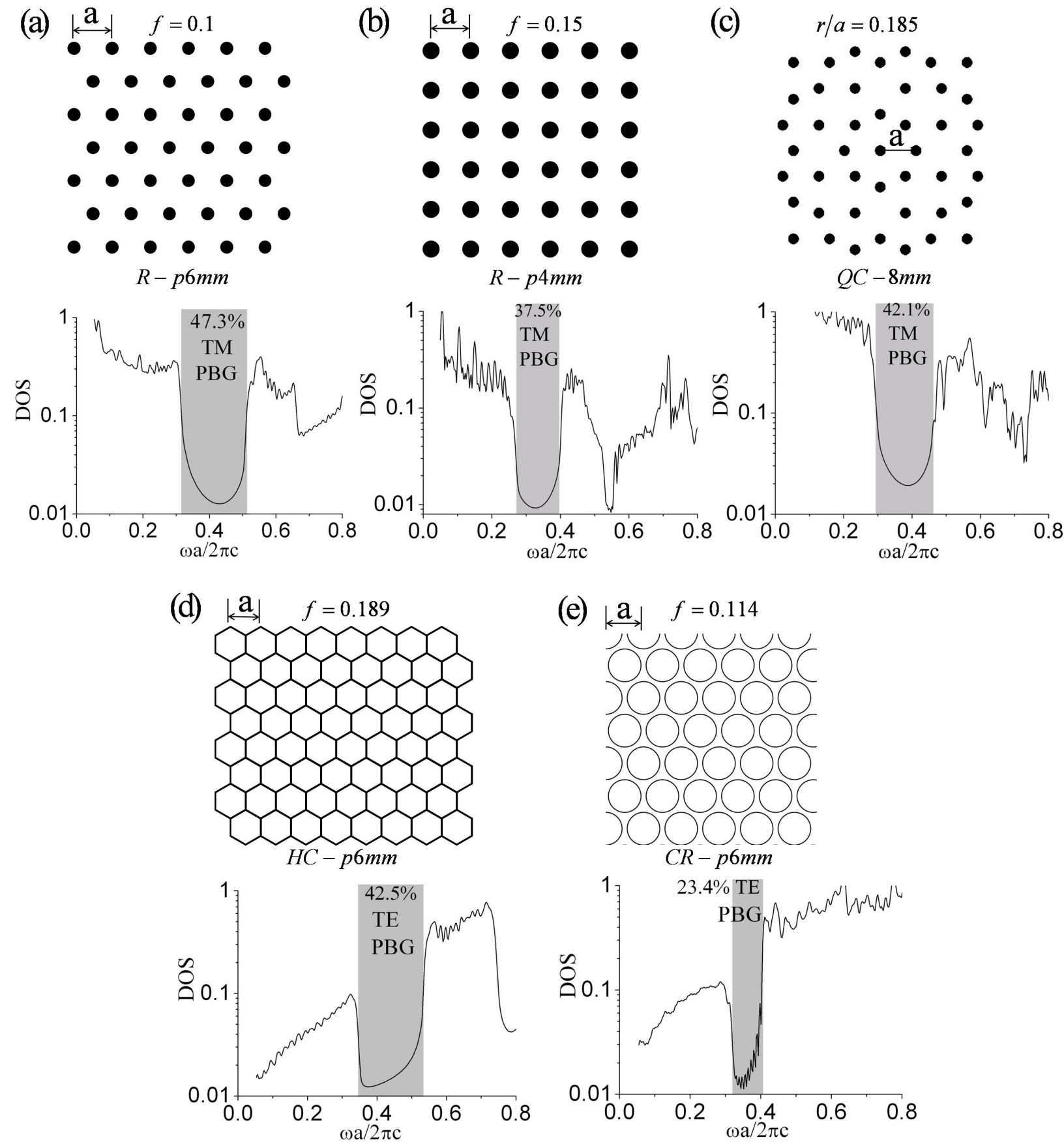
(a)
a
f = 0.1
R – p6mm
47.3%
TM
PBG
DOS
ωa/2πc
(b)
a
f = 0.15
R – p4mm
37.5%
TM
PBG
DOS
ωa/2πc
(c)
r/a = 0.185
a
QC – 8mm
42.1%
TM
PBG
DOS
ωa/2πc
(d)
a
f = 0.189
HC – p6mm
42.5%
TE
PBG
DOS
ωa/2πc
(e)
a
f = 0.114
CR – p6mm
23.4% TE
PBG
DOS
ωa/2πc

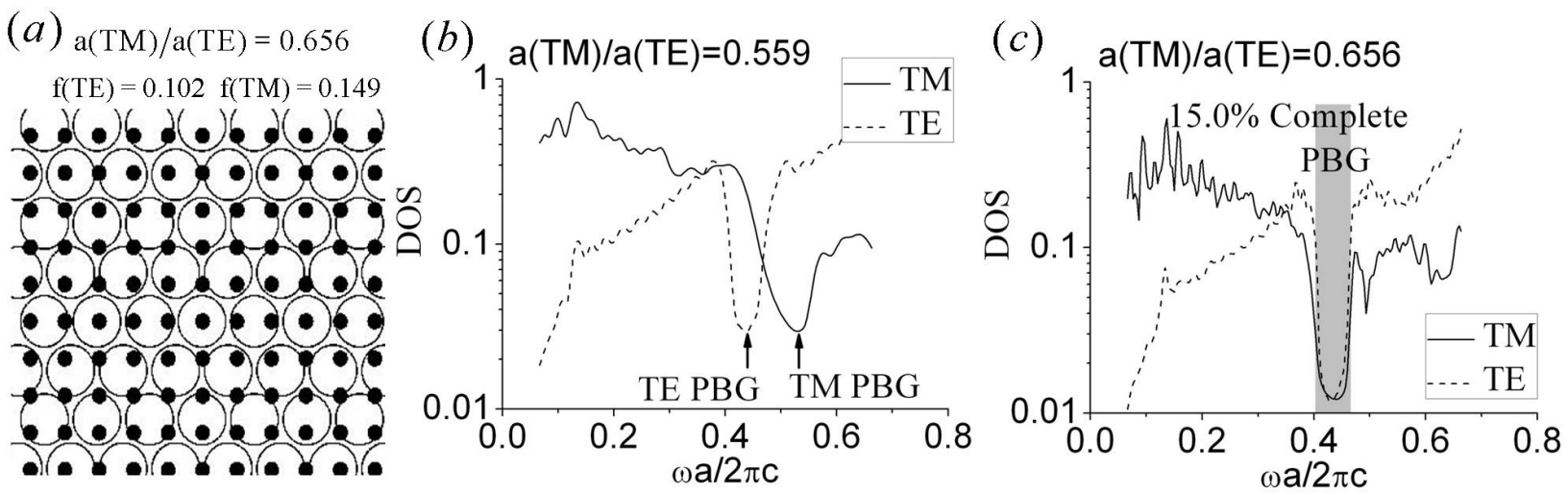
(a)
a(TM)/a(TE) = 0.656
f(TE) = 0.102 f(TM) = 0.149
(b)
a(TM)/a(TE)=0.559
TM
TE
DOS
1
0.1
0.01
TE PBG
TM PBG
0.0
0.2
0.4
0.6
0.8
ωa/2πc
(c)
a(TM)/a(TE)=0.656
15.0% Complete
PBG
TM
TE
DOS
1
0.1
0.01
0.0
0.2
0.4
0.6
0.8
ωa/2πc

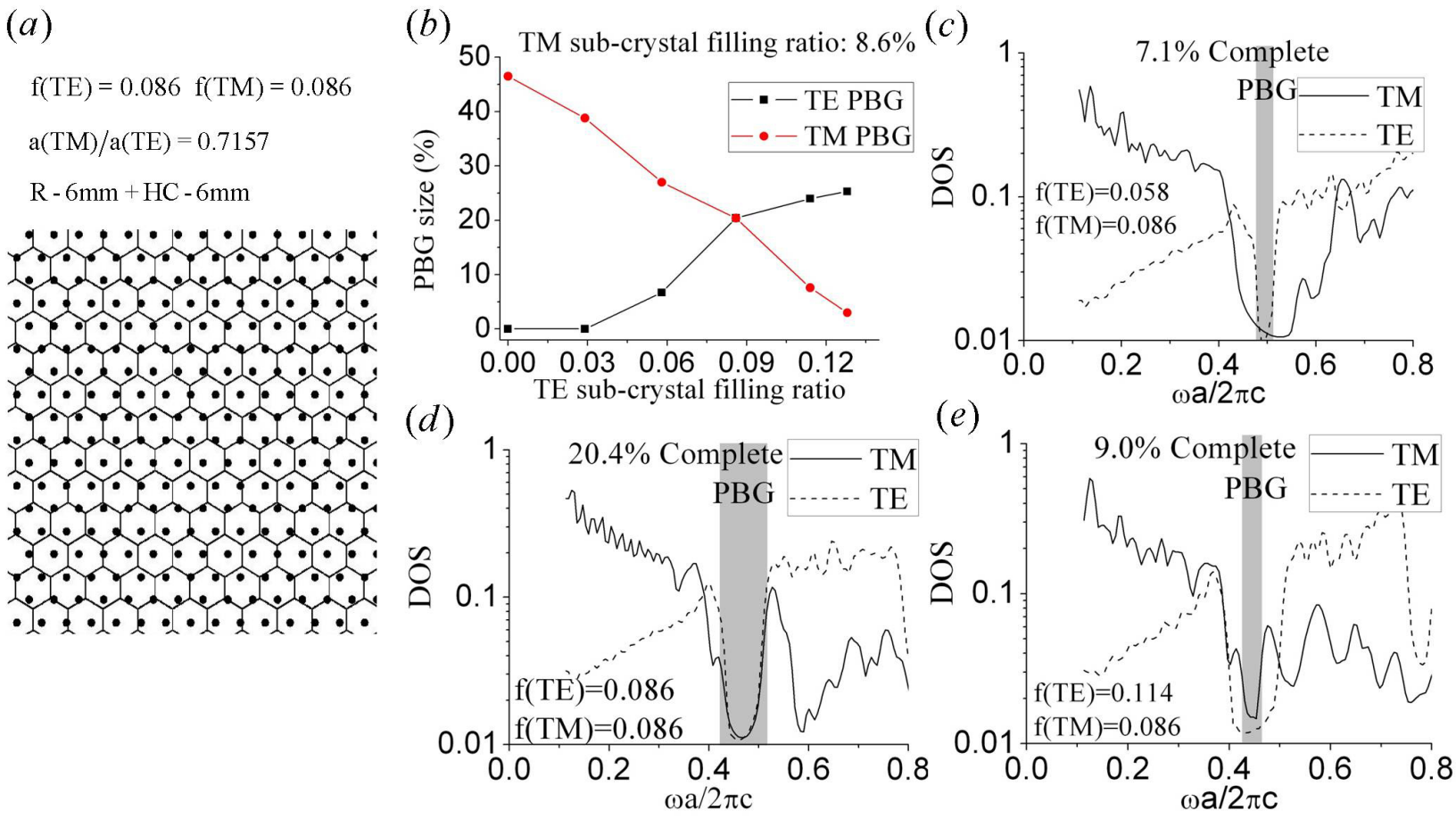
(a)
f(TE) = 0.086 f(TM) = 0.086
a(TM)/a(TE) = 0.7157
R - 6mm + HC - 6mm
(b)
TM sub-crystal filling ratio: 8.6%
TE PBG
TM PBG
PBG size (%)
TE sub-crystal filling ratio
(c)
7.1% Complete PBG
TM
TE
f(TE)=0.058
f(TM)=0.086
DOS
ωa/2πc
(d)
20.4% Complete PBG
TM
TE
f(TE)=0.086
f(TM)=0.086
DOS
ωa/2πc
(e)
9.0% Complete PBG
TM
TE
f(TE)=0.114
f(TM)=0.086
DOS
ωa/2πc

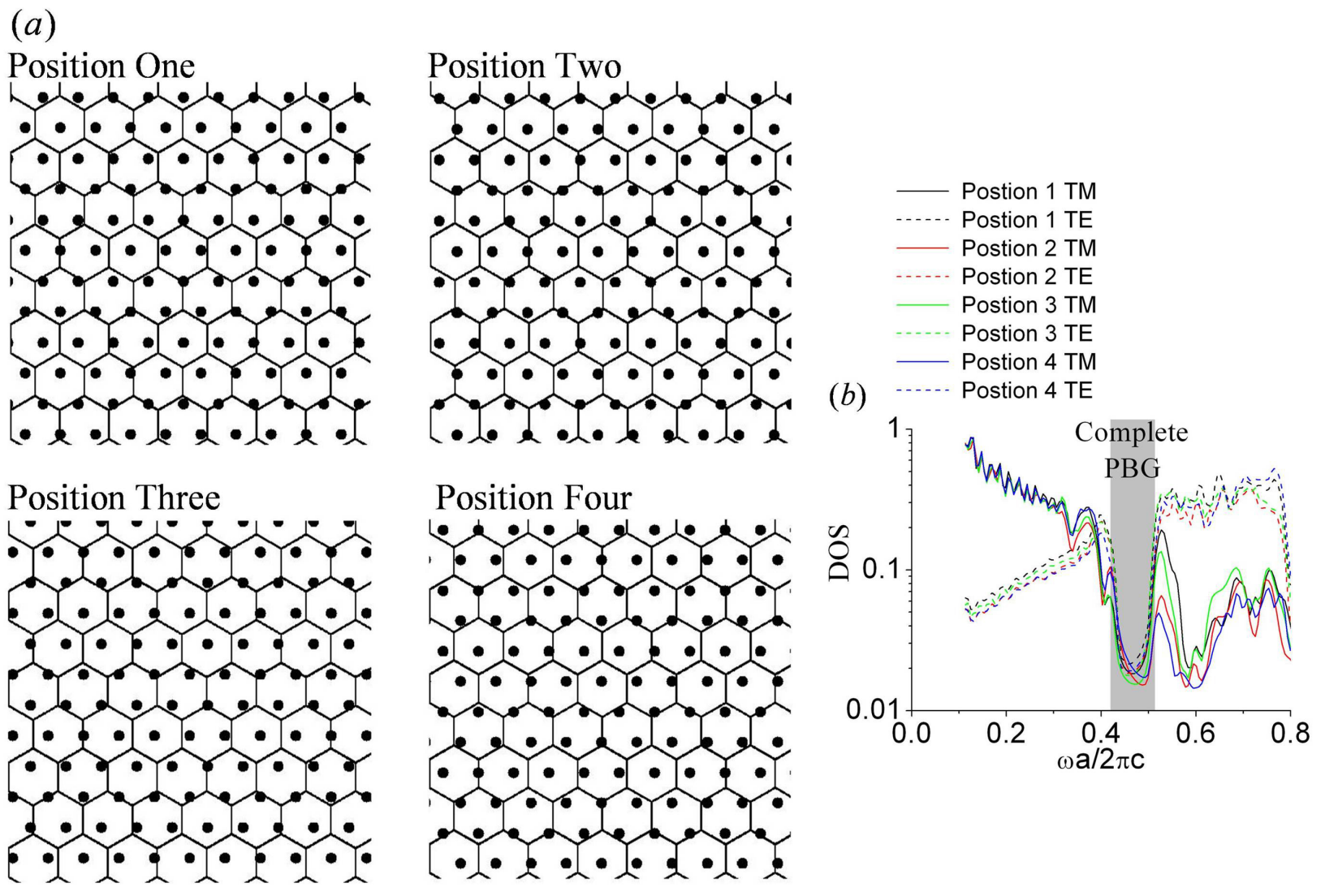
(a)
Position One
Position Two
Position Three
Position Four
(b)
Postion 1 TM
Postion 1 TE
Postion 2 TM
Postion 2 TE
Postion 3 TM
Postion 3 TE
Postion 4 TM
Postion 4 TE
Complete
PBG
DOS
1
0.1
0.01
0.0
0.2
0.4
0.6
0.8
ωa/2πc

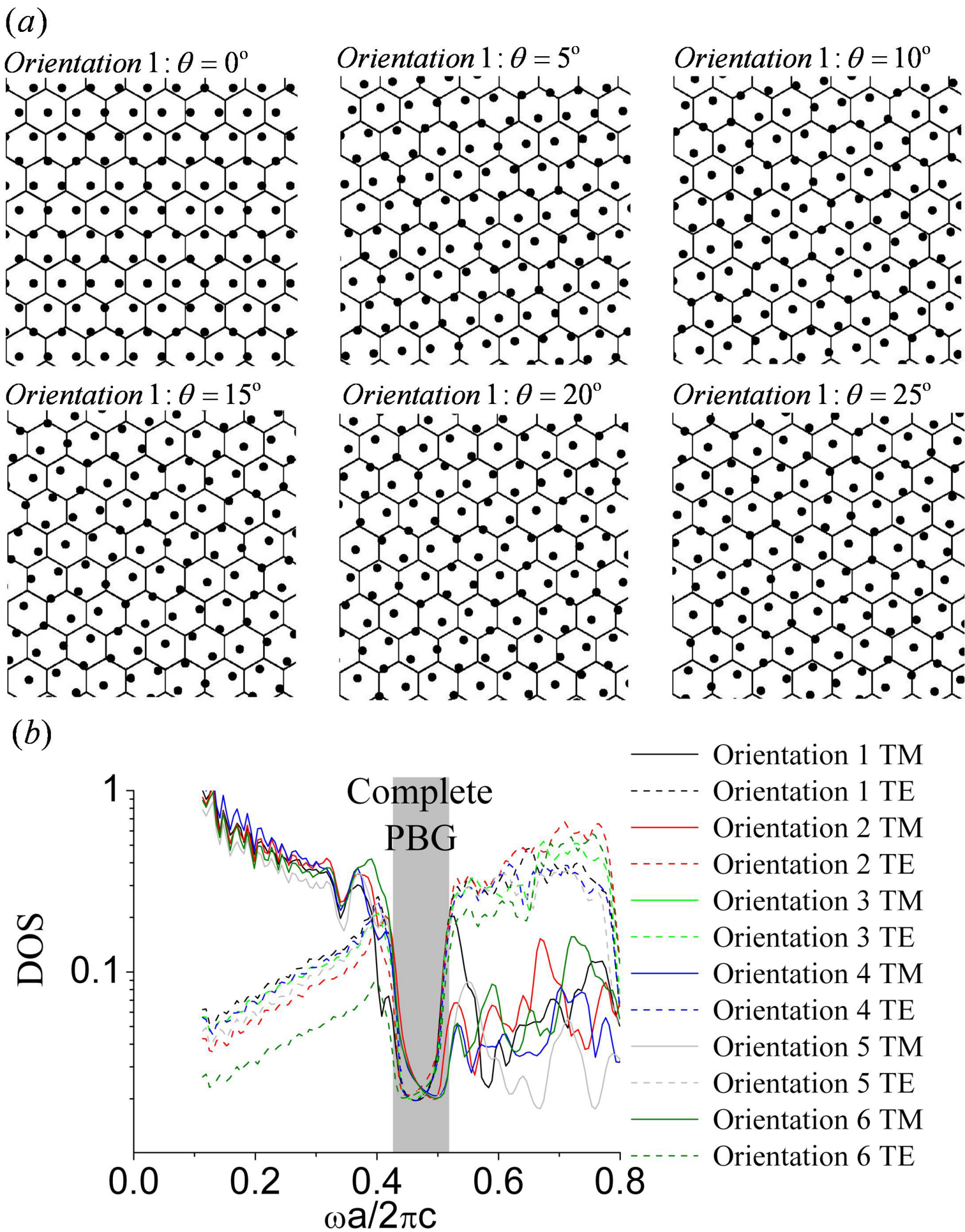
(a)
Orientation 1 : θ = 0°
Orientation 1 : θ = 5°
Orientation 1 : θ = 10°
Orientation 1 : θ = 15°
Orientation 1 : θ = 20°
Orientation 1 : θ = 25°
(b)
Complete
PBG
DOS
1
0.1
0.0
0.2
0.4
0.6
0.8
ωa/2πc
Orientation 1 TM
Orientation 1 TE
Orientation 2 TM
Orientation 2 TE
Orientation 3 TM
Orientation 3 TE
Orientation 4 TM
Orientation 4 TE
Orientation 5 TM
Orientation 5 TE
Orientation 6 TM
Orientation 6 TE

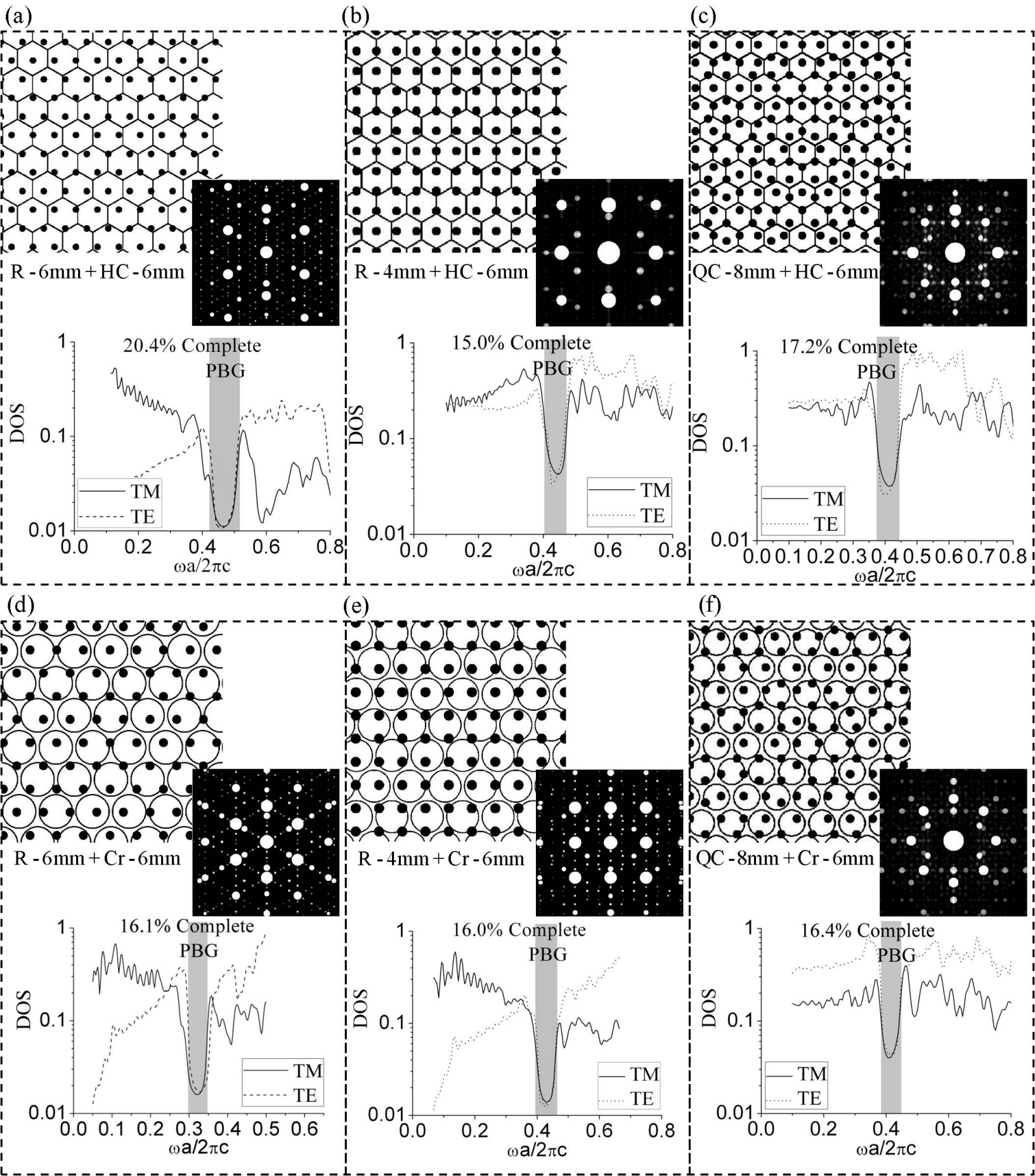
(a)
R - 6mm + HC - 6mm
20.4% Complete
PBG
DOS
TM
TE
ωa/2πc
(b)
R - 4mm + HC - 6mm
15.0% Complete
PBG
DOS
TM
TE
ωa/2πc
(c)
QC - 8mm + HC - 6mm
17.2% Complete
PBG
DOS
TM
TE
ωa/2πc
(d)
R - 6mm + Cr - 6mm
16.1% Complete
PBG
DOS
TM
TE
ωa/2πc
(e)
R - 4mm + Cr - 6mm
16.0% Complete
PBG
DOS
TM
TE
ωa/2πc
(f)
QC - 8mm + Cr - 6mm
16.4% Complete
PBG
DOS
TM
TE
ωa/2πc

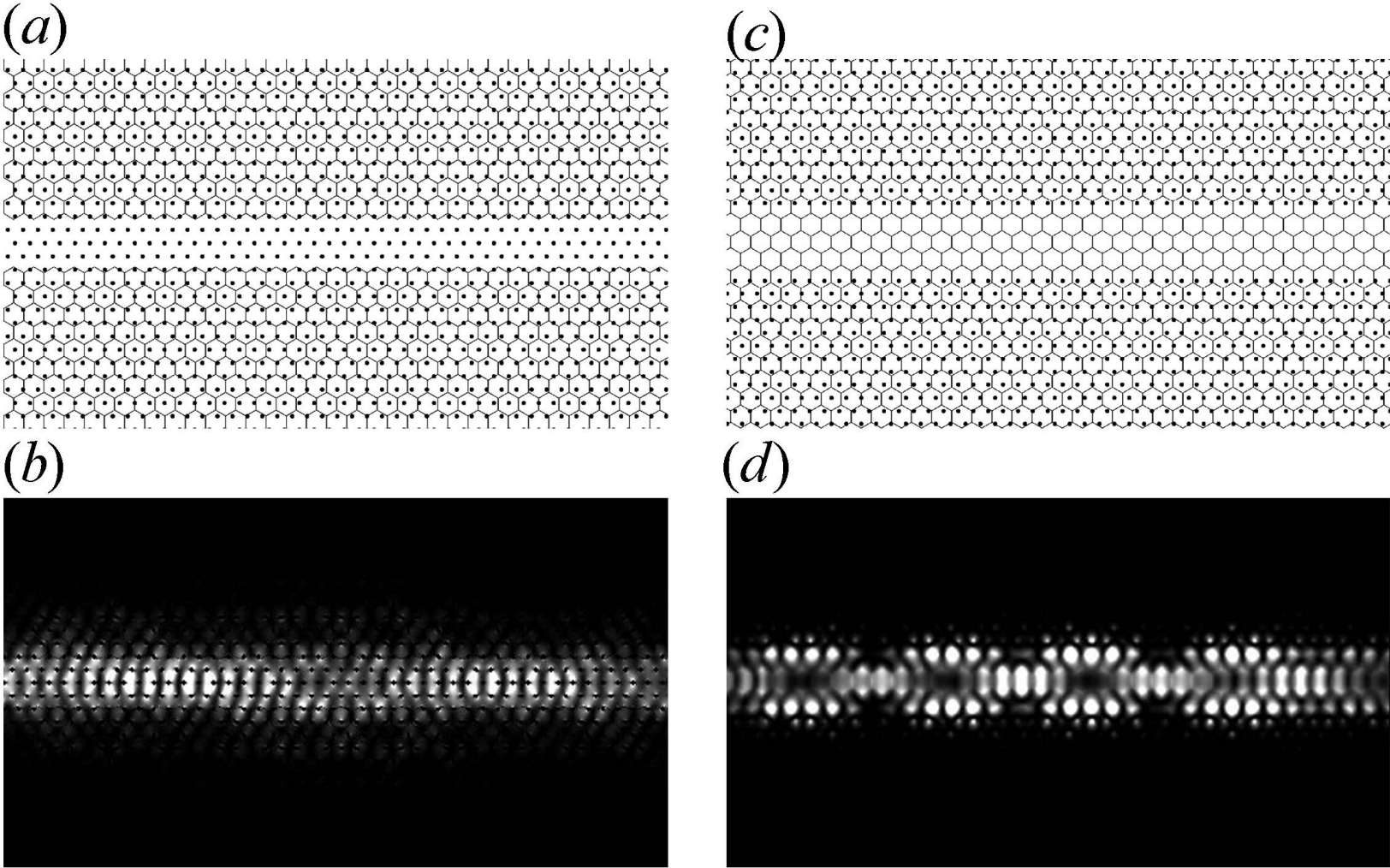
(a)
(c)
(b)
(d)